Vibrational substructure in the OH stretching band of water

ARTICLE *in* CHEMICAL PHYSICS LETTERS · SEPTEMBER 2003

Impact Factor: 1.9 · DOI: 10.1016/S0009-2614(03)01267-3

4 AUTHORS:

Zhaohui Wang
Xiamen University
34 PUBLICATIONS **1,066** CITATIONS
SEE PROFILE

Andrei V. Pakoulev
University of Wisconsin–Madison
36 PUBLICATIONS **620** CITATIONS
SEE PROFILE

Yoonsoo Pang
Gwangju Institute of Science and Tech…
28 PUBLICATIONS **528** CITATIONS
SEE PROFILE

Dana D Dlott
University of Illinois, Urbana-Champaign
297 PUBLICATIONS **6,640** CITATIONS
SEE PROFILE

Available online at www.sciencedirect.com
SCIENCE DIRECT®
Chemical Physics Letters 378 (2003) 281–288
CHEMICAL PHYSICS LETTERS
www.elsevier.com/locate/cplett

Vibrational substructure in the OH stretching band of water

Zhaohui Wang, Andrei Pakoulev, Yoonsoo Pang, Dana D. Dlott *

School of Chemical Sciences, University of Illinois at Urbana-Champaign, Box 01-6 CLSL, 600 S. Mathews Avenue, Urbana, IL 61801, USA

Received 10 June 2003; in final form 2 July 2003

Abstract

Spectral diffusion in the OH stretching (ν_{OH}) band of water is studied by ultrafast IR-Raman spectroscopy. The ν_{OH} transition consists of two overlapping inhomogeneously broadened subbands, a broader ($\sim$500 cm^{-1}) redshifted band and a smaller, narrower ($\sim$200 cm^{-1}) blueshifted band. The blueshifted band, which shows less spectral diffusion, has a longer lifetime (0.75 vs 0.55 ps) and a smaller vibrational frequency blueshift from the ground state (65 vs 90 cm^{-1}), is tentatively assigned to water molecules where one hydrogen atom has a broken hydrogen bond.

1. Introduction

In this work, we use ultrafast IR-Raman spectroscopy [1], a type of 3D vibrational spectroscopy [2], to investigate subband structures in the OH stretching band (ν_{OH}) of water. In the past few years, ultrafast mid-IR hole-burning spectroscopies have been used to study spectral diffusion within ν_{OH} ($\sim$3000–3600 cm^{-1}) of the HOD solute in D_2O solvent [3–9]. A combination of experiment and related theoretical work [10–17] has now demonstrated that spectral diffusion on the >50 fs time scale probed by experiments so far, is caused by the forming and breaking of hydrogen bonds.

Only recently has ultrafast vibrational spectroscopy been applied to ν_{OH} of water [9,18–22]. There are similarities and differences between HOD/D_2O and water. The hydrogen-bonding dynamics of the two are presumably quite similar [12]. The vibrational spectra are quite different. In HOD there are three separate bands, ν_{OH}, the OD stretch ν_{OD}, and the bend overtone $2\delta_{HOD}$. In water there is a single band, a mixture of symmetric ν_{OH}, antisymmetric ν_{OH} and $2\delta_{H_2O}$. The vibrational relaxation (VR) pathways are also quite different, as a consequence of this different level structure [9,10,23,24]. Ultrafast mid-IR experiments in HOD probe an excitation localized mainly on the OH group [12], whereas water experiments probe a ν_{OH} that is delocalized over the entire molecule. Due to its high absorption coefficient [25], pump–probe experiments in water necessarily involve a bulk temperature jump ($\Delta T = 30$ K is typical [19,20] but the boiling point 373 K is easily reached), which is not a factor in dilute HOD/D_2O.

* Corresponding author. Fax: +1-217-244-3186.
E-mail address: dlott@scs.uiuc.edu (D.D. Dlott).

0009-2614/$ - see front matter © 2003 Elsevier B.V. All rights reserved.
doi:10.1016/S0009-2614(03)01267-3

The large widths (FWHM ~400–500 cm^{-1}) of the v_{OH} bands of HOD and water are caused by a distribution of hydrogen bond strengths. The weaker hydrogen-bonded sites absorb near the blue edge, and the stronger sites absorb near the red edge. A widespread notion (see, e.g. [6,12,16]) has been the idea of a linear 1:1 relationship between hydrogen bond strength and v_{OH} transition frequency. Recently two independent calculations using mixed classical and quantum simulation techniques, by Lawrence and Skinner [11,12] and by Rey and Hynes [16], have shown there is indeed a reasonable correspondence between the v_{OH} frequency and the hydrogen bond strength. However, this correspondence is not 1:1 and there is considerable dispersion, so that the v_{OH} transitions for different hydrogen-bonded configurations are broad and overlapping.

An important question not convincingly answered by either experiment or theory is whether ultrafast vibrational spectroscopy can resolve different hydrogen-bonded configurations within the broad v_{OH} band. In 1998, Laenen et al. [3,4] interpreted their two-color mid-IR pump–probe measurements on HOD/D_2O in terms of three distinct Gaussian subbands, termed (I)–(III), which were believed to arise from distinctly different hydrogen-bonded configurations. On the basis of comparisons to Rahman and Stillinger's 1971 simulations [26], these bands were assigned to (I) 'ice-like', (II) 'bridged', and (III) 'bifurcated' hydrogen-bonded sites.

In HOD/D_2O experiments by other groups, this subband picture was ignored in favor of a continuous distribution picture, where v_{OH} dynamics were explained in terms of spectral diffusion plus a wavenumber-dependent VR lifetime. The spectral diffusion [5,6] involved hydrogen bond dynamics plus what Woutersen and Bakker [5] in 1999 termed a time-dependent 'vibrational Stokes shift'. The vibrational Stokes shift is formally the energy difference between the $v = 0 \rightarrow 1$ transition and the $v = 1 \rightarrow 0$ transition [13], and it is expected to be a redshift due to stronger hydrogen bonding in the $v = 1$ state. The measured redshift was 70 cm^{-1} [5], and subsequently Lawrence and Skinner calculated 57 cm^{-1} [13]. A weakly wavenumber-dependent lifetime was reported by Bakker's group in 1997 [27]. Laenen et al. [3] criticized this interpretation, pointing out that transients at different probe wavenumbers actually see an effective time constant τ which includes T_1 and spectral diffusion. Gale et al. [28] reported that T_1 increased from 0.5 to 1.0 ps moving from the red edge to the blue edge of the v_{OH} band using two different methods of analysis, the single-frequency pump–probe technique or the total area of the induced absorption.

Spectral diffusion of water was first studied by the Dlott group in 2000 [9]. We reported that $T_1 \sim 1$ ps, and observed that VR of v_{OH} produced between one and two quanta of δ_{OH}. The spectral diffusion of water on the >500 fs time scale involved primarily 'uphill' spectral diffusion from the red to the blue [9,22]. This net movement to the blue raises the possibility that the energy shift between the ground and excited states might be a blueshift in water. Bakker's group in 2001 and 2002 [19,20] proposed a different interpretation of water VR. Their mid-IR transients displayed two time constants, 0.26 and 0.55 ps. The 0.26 ps time constant was attributed to T_1 and the 0.55 ps time constant to ground state recovery from an intermediate state, possibly δ_{H_2O}. Subsequently our group used anti-Stokes probing methods to show that the faster time constant was really due to uphill spectral diffusion, and the slower time constant was really T_1 [22].

In our view, the question of whether vibrational subbands corresponding to different hydrogen-bonded configurations can be resolved within the v_{OH} transition of HOD/D_2O has not been answered convincingly. We believe that different configurations in water should have even more dispersion than in HOD. The v_{OH} transition frequency in water should be affected by the configurational disorder at both H atoms, while the v_{OH} transition in HOD is not strongly affected by configurational disorder at the D atom [12]. Since v_{OH} transitions corresponding to different configurations are broad and overlapping, ordinary vibrational spectroscopy clearly cannot distinguish subband structure. However, three-dimensional techniques such as two-color IR and IR-Raman used here provide more information. Tuning the pump pulse could affect the relative intensities of different subbands [3], and different subbands

might evidence different spectral diffusion, different VR lifetimes, and different vibrational Stokes shifts. It is this question, the existence of vibrational subbands, that is the main issue addressed by the present work. Along the way, we have also made the most precise measurements so far of the water vibrational lifetime and the vibrational Stokes shift.

2. Experimental

The experimental arrangement for IR-Raman studies of water has been described previously [9,18]. A tunable mid-IR pulse (25 cm^{-1} bandwidth, 370 μm diameter, ~0.7 ps) pumps a selected region of ν_{OH}. A 532 nm visible Raman probe pulse (15 cm^{-1} bandwidth, 400 μm diameter, ~0.7 ps, 20 μJ) generates an anti-Stokes spectrum detected by a multichannel spectrograph [18]. The anti-Stokes signal is proportional to the Raman cross-section multiplied by the excited state population [1]. Differences between the anti-Stokes Raman and IR probe methods have been discussed in detail in a previous Letter [22]. Recently we have developed a new laser [22] that has resulted in a considerable improvement in sensitivity over previous [9] work. Since our most recent study of water [22], we have also improved our pulse compression, leading to an ~60% improvement in time resolution.

In the IR-Raman technique, a coherent artifact may be generated by non-linear light scattering (NLS) [9,18,29] at frequency $\omega_{IR} + \omega_{vis}$. In our anti-Stokes spectra, this artifact appears at the same wavenumber as the pump pulse. The time dependence of the NLS artifact, which arises from a coherent interaction of the pump and probe pulses, is used to characterize the apparatus time response [22].

Of particular concern in water experiments is the bulk temperature jump ΔT. We can accurately calculate ΔT knowing the pump pulse fluence J and the water absorption coefficient α [22]. The pump pulse intensity was adjusted to give $\Delta T = 30 \pm 2$ K (i.e., 293 K → 323 K) at each pump wavenumber unless otherwise indicated. For example with 3115 cm^{-1} pumping where $\alpha = 4640$ cm^{-1} [25], the mid-IR energy was 25 μJ with a beam diameter of 370 μm. More pump pulse energy is needed to produce the same ΔT on the absorption edge, so at constant ΔT we obtain a better signal-to-noise ratio with absorption edge pumping.

3. Results

Fig. 1 shows the Stokes Raman spectrum of ν_{OH} plus three representative anti-Stokes transient spectra at $t = 1$ ps, with pumping near the red edge ($\omega_{IR} = 3115$ cm^{-1}), the line center ($\omega_{IR} = 3315$ cm^{-1}) or the blue edge ($\omega_{IR} = 3500$ cm^{-1}). The sharper peak that appears at the pump wavenumber is the NLS artifact. Its spectral width of 35 cm^{-1} is the convolution of the pump and probe pulse widths. The fitted curves in each panel are the sum of two Gaussian subbands plus one Gaussian for the NLS artifact. Fig. 1 shows that the population distribution of $v = 1$ excitations can be shifted quite a bit to the red or to the blue by tuning the pump pulse.

A complete time-sequence of spectra was obtained with red edge 3115 cm^{-1} pumping, where our signal-to-noise ratio is optimal. Fig. 2 shows a few of these time-dependent spectra. A particularly

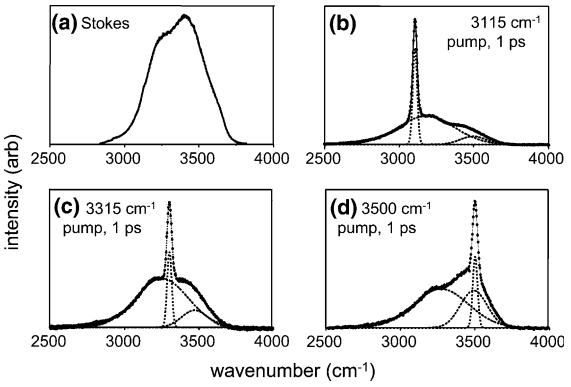

Fig. 1. (a) Stokes Raman spectrum of water at ambient temperature. (b–d) Anti-Stokes transient spectra at 1 ps delay time, pumped on the red edge, band center, and blue edge. The sharp feature is the NLS artifact. The data are fit by the sum of two overlapping Gaussian subbands, a broader red and a narrower blue subband ν_{OH}^{R} and ν_{OH}^{B}, plus one Gaussian for the NLS artifact.

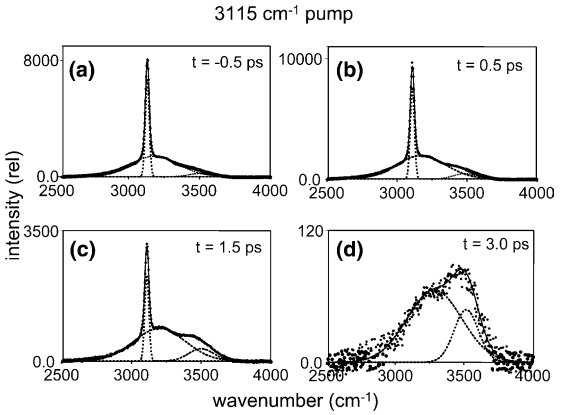

Fig. 2. A time series of transient spectra with 3115 cm^{-1} red edge pumping, fit using the two Gaussian subbands ν^{R}_{OH} and ν^{B}_{OH}.

simple way of analyzing these data is to look at the time-dependent intensity within different wavenumber regions. Using a 50 cm^{-1} window and skipping the region near the NLS artifact, we see approximately exponential decays that yield wavenumber-dependent relaxation time constants τ. As shown in Fig. 3, τ varies smoothly from $\sim$0.35 ps on the red edge to $\sim$0.75 ps on the blue edge.

In the spirit of Laenen et al. [3,4], we also fit our spectra with Gaussian subbands, using subroutines in the MicroCal Origin™ software package. We found that all our transient spectra could be fit quite accurately using just two Gaussian functions plus one Gaussian for the NLS artifact. The NLS part was always centered at the pump wavenumber and its FWHM of 33 ± 3 cm^{-1} was delay time independent. As shown in Figs. 1 and 2, the two remaining overlapping Gaussian subbands consisted of a broader band (FWHM $\sim$500 cm^{-1}) centered near 3200 cm^{-1} which spans almost the entire ν_{OH} region plus a narrower band (FWHM $\sim$200 cm^{-1}) centered near 3500 cm^{-1}. We will call these two subbands the 'red' and 'blue' subbands [22], ν^{R}_{OH} and ν^{B}_{OH}.

With ν^{R}_{OH} pumping, ν^{R}_{OH} rises instantaneously but ν^{B}_{OH} has a delayed rise (Figs. 2a–c). It is not possible to find a pump wavenumber in the ν_{OH} band that does not excite ν^{R}_{OH} directly. When the pump is tuned to the center of ν^{B}_{OH} near 3500 cm^{-1} (Fig. 1d), both ν^{R}_{OH} and ν^{B}_{OH} rise instantaneously.

Fig. 4 shows the behavior of the peak and FWHM of the two subbands with different pump wavenumbers. The broader ν^{R}_{OH} undergoes uphill spectral diffusion as time passes. As we showed earlier, there is more uphill diffusion with increasing pump pulse energy [22], so the uphill diffusion is driven – at least in part – by the generation of excitations, including δ_{H_2O}, produced by ν_{OH} decay. Fig. 4 shows that the initial location of

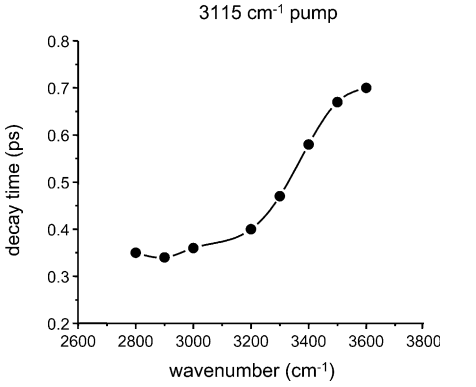

Fig. 3. The effective decay lifetime τ of the excited state population in 50 cm^{-1} bands at the indicated wavenumber, using 3115 cm^{-1} pumping.

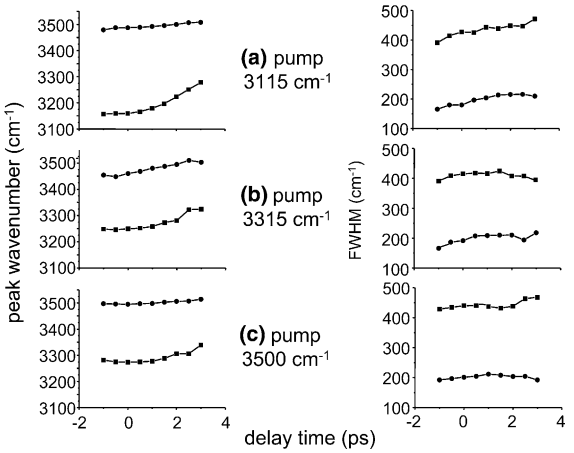

Fig. 4. The time dependence of the peak center and FWHM of the two Gaussian subbands, pumped near the red edge, the band center, and the blue edge. Regardless of the pump wavenumber, ν^{R}_{OH} tends toward 3325 cm^{-1} and ν^{B}_{OH} towards 3525 cm^{-1} at longer time.

the ν_{OH}^{R} peak can be shifted from 3150 to 3300 cm^{-1} by tuning the pump pulse from the red edge to the blue edge. However, as time passes, the ν_{OH}^{R} peak always ends up near 3325 cm^{-1}. Whether ν_{OH}^{R} is pumped on its red or blue edges, it broadens as it shifts, but when ν_{OH}^{R} is pumped near its peak, it hardly broadens at all. The time-dependent uphill spectral shift of ν_{OH}^{B} is much smaller. The ν_{OH}^{B} starting location can be varied only from 3450 to 3500 cm^{-1}. Regardless of the pump wavenumber, the ν_{OH}^{B} peak always ends up near 3525 cm^{-1}. The ν_{OH}^{B} FWHM can be varied only in a narrow range between 175 and 200 cm^{-1}.

In the past, there has been some discussion whether narrow peaks such as the one we attribute to an NLS artifact might actually be narrow holes burnt into the ν_{OH} band by the pump pulse [3,4,9,30]. Our present results appear conclusive on this point. If there were a narrow hole with for instance 3115 cm^{-1} pumping, it ought to move to the red and broaden like the rest of the ν_{OH}^{R} subband. However, the narrow peak does not move or broaden substantially, so there is no narrow hole burnt into the ν_{OH} band.

The time dependence of the areas of the two subbands with 3115 cm^{-1} pumping is shown in Fig. 5. The right-hand side of Fig. 5 shows data taken at twice the pump intensity used for the other experiments, where $\Delta T = 58$ K and the final temperature of 331 K remains below the boiling point. Fig. 5 tells a much different story than Fig. 3. The time dependence of the NLS artifact which characterizes the apparatus time response, is accurately fit by a Gaussian function with FWHM of 1.1 ± 0.1 ps. The red subband ν_{OH}^{R}, which is directly excited by the 3115 cm^{-1} pump pulse, rises instantaneously. The ν_{OH}^{R} data were fit using the convolution of the apparatus response plus an exponential decay, yielding a lifetime $T_1 = 0.55 \pm 0.05$ ps. The blue subband ν_{OH}^{B}, which is not directly pumped by a 3115 cm^{-1} pulse, has a delayed rise. The ν_{OH}^{B} data were fit using the convolution of the apparatus response with a 0.55 ps exponential build up and an exponential decay. The ν_{OH}^{B} lifetime was $T_1 = 0.75 \pm 0.05$ ps. Although the data were noisier, the same ν_{OH}^{R} and ν_{OH}^{B} lifetimes were obtained with $\Delta T = 15$ K, but when $\Delta T = 60$ K was used (Fig. 5b), the ν_{OH}^{B} lifetime increased by 15%.

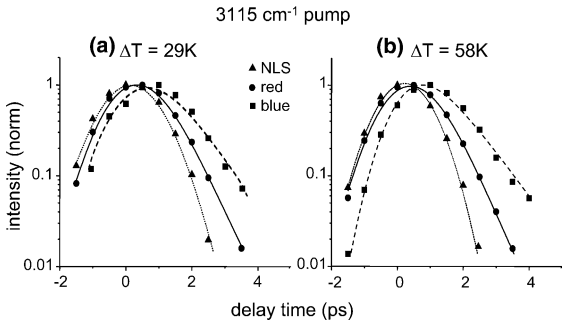

Fig. 5. Time dependence with 3115 cm^{-1} pumping, of the areas of the NLS artifact and the red and blue subbands. The areas are all normalized to the same peak.

4. Discussion

In this section we will discuss the vibrational lifetime T_1 and the vibrational Stokes shift of water. Then we will discuss the nature of the two subbands observed in the water ν_{OH} transient spectra.

4.1. Vibrational lifetime T_1

The red subband has $T_1 = 0.55 \pm 0.05$ ps and the blue subband has $T_1 = 0.75 \pm 0.05$ ps. T_1 for ν_{OH}^{B} is seen to grow longer when ΔT is greater than 30 K. The $T_1 = 0.75$ value obtained here for ν_{OH}^{B} is more reliable than the $T_1 = 1.1$ ps value we measured in [22], since that study used longer duration pulses and larger values of ΔT. Lock and Bakker's IR experiments on water [19,20] saw two time constants, 0.26 and 0.55 ps, which were assigned to T_1 and ground state repopulation, respectively. These time constants were obtained by time scans at fixed IR probe wavenumbers, which is tantamount to what we did in Fig. 3. Fig. 3 shows that the apparent decay constant τ ranges from 0.35 ps on the red edge to 0.75 ps on the blue edge. The 0.35 ps value is not T_1, but rather is a combination of T_1 plus uphill spectral diffusion plus ν_{OH}^{R} broadening. The predominant effect in this triad is the spectral diffusion, so 0.35 ps is a reasonable estimate for the spectral diffusion time constant. It

is clear that the time constants obtained by Lock and Bakker are effective time constants that combine the effects of population relaxation and spectral diffusion. The subband analysis technique looks only at the decay of the subband area regardless of its peak shift or broadening, which allows us to entirely separate the lifetime T_1 from spectral diffusion.

4.2. Vibrational Stokes shift

With Raman probing, the vibrational Stokes shift should be the energy difference between the Stokes Raman spectrum ($v = 0 \rightarrow 1$) and the anti-Stokes spectrum ($v = 1 \rightarrow 0$) transition [9]. It is not immediately obvious how to reconcile the subband picture of Laenen et al. [3,4] with the Stokes shift picture, since different subbands could have different shifts, and meanwhile the excited state subband peak frequencies depend on pump wavenumber and are moving targets due to spectral diffusion. However, now we can clearly see how to do this for water. We see two major subbands in both the Stokes and the anti-Stokes spectra and we have fully characterized the time-dependent spectral diffusion of each subband. By fitting the two major subbands in the Stokes spectrum in Fig. 1a, we obtained peak values of 3235 and 3460 cm^{-1}. The anti-Stokes data in Fig. 4 show that the red subband tends toward 3325 cm^{-1} and the blue subband tends toward 3525 cm^{-1}, regardless of the pump wavenumber. Since these extrapolations are only approximate, we will estimate an error of ± 10 cm^{-1} for the anti-Stokes data. Thus the vibrational Stokes shift for both bands is a blueshift in water. For ν_{OH}^{R}, $\Delta\nu_{st} = -90 \pm 10$ cm^{-1} and for ν_{OH}^{B}, $\Delta\nu_{st} = -65 \pm 10$ cm^{-1}. These results for the two subbands appear to be clearly different.

4.3. Vibrational substructure

The Stokes Raman spectrum of water is usually fit by four Gaussian subbands [31], two larger bands for the two major peaks in Fig. 1a, and much smaller bands at the red and blue edges. However, only two subbands were needed to fit our anti-Stokes transient data at all times and all pump wavenumbers. This could result from more dispersion in the spectrum of different hydrogen-bonded configurations in the $v = 1$ state compared to the $v = 0$ state of ν_{OH}, or alternatively we never tuned the pump pulses far enough to the extreme edges of the ν_{OH} absorption to produce much population in the edge bands. The inhomogeneous nature of the ν_{OH}^{R} and ν_{OH}^{B} subbands is clearly revealed by Fig. 4, which shows that the peak locations and widths can be changed by tuning the pump wavenumber. So our data compel us to believe in two inhomogeneously broadened subbands in water, but do not rule out the possibility of other much smaller subbands. Laenen's three subbands in HOD [3] are quite a bit narrower than our water subbands, which have FWHM of 500 and 200 cm^{-1}. Laenen's subbands, centered at 3330 cm^{-1} ('ice-like'), 3400 cm^{-1} ('bridged') and 3500 cm^{-1} ('bifurcated'), had FWHM of 40, 80, and 80 cm^{-1}.

The recent calculations of HOD [12,16] show that it is dangerous to infer too much about the water structure from the vibrational spectrum. Nevertheless we will now do so. There is something obviously special about ν_{OH}^{B}, that distinguishes it from the rest of the vibrational spectrum. It has a smaller Stokes shift and little spectral diffusion. Increasing ΔT generates more of ν_{OH}^{B} from ν_{OH}^{R} [22]. The spectrum of ν_{OH}^{B} looks a great deal like the ν_{OH} frequency distribution of non-hydrogen-bonded HOD from Lawrence and Skinner's calculations shown in Fig. 6 of [12]. In fact the similarity is truly striking. Thus the blue subband ν_{OH}^{B} is proposed to represent water with a single H atom that is not hydrogen bonded. The width of ν_{OH}^{B} is due to dispersion in the other hydrogen bond lengths, angles, etc.

The average number of hydrogen bonds in water is 3.58, meaning ~58% of water molecules have four hydrogen bonds and ~40% have three hydrogen bonds. Of the ~40% with one broken bond, ~20% have one H atom with a broken hydrogen bond. It would be nice to look at the fits in Figs. 1 and 2 to see if ν_{OH}^{B} comprised 21% of the total area; however, the ratio of ν_{OH}^{B} to ν_{OH}^{R} areas is not in equilibrium and depends on the pump wavenumber. Nevertheless our data are not inconsistent with 21%. If our interpretation of ν_{OH}^{B} is

correct, its decay rate should be the sum of the VR rate plus the rate for spontaneously reforming the broken hydrogen bond. With an incoherent anti-Stokes probe, it does not matter if the hydrogen bond remains continuously broken, so the relevant rate would be the 'intermittent' rate for spontaneously reformation [32,33]. A quite recent calculation of the lifetime (the inverse of the constant denoted k' [32]) from Berne's group [34] using several different water potential energy surfaces gives values ranging from 1.0 to 1.5 ps, which indicates that hydrogen bond reformation and VR are both significant v_{OH}^{B} decay mechanisms. The equilibrium shifts toward more broken hydrogen bonds at higher temperature, which would account for the lifetime increase of v_{OH}^{B} with increasing ΔT. It might be possible to extract the rate for spontaneous hydrogen bond reformation by watching the blue subband decay into the red subband, but this will be difficult since we cannot pump only v_{OH}^{B} without also pumping v_{OH}^{R}.

The broader v_{OH}^{R}, which has amplitude throughout the v_{OH} band, would in this picture represent all configurations for which both H atoms are hydrogen bonded, including configurations where O atoms have a broken hydrogen bond. The much greater width of this dominant subband than anything that has been proposed for HOD [3,4], indicates that the vibrational transitions of all these different configurations in water overlap a great deal. As explained in Section 1, this appears to be a consequence of the sensitivity of water stretching vibrations to configurational disorder at both H atoms. Although dilute solutions are more difficult for the insensitive Raman probe method, we hope to soon use the anti-Stokes probe technique to reexamine the question of subbands in HOD/D_2O.

5. Concluding remarks

Our data clearly show that the water v_{OH} Raman spectrum can be explained by two overlapping subbands with different spectral diffusion, different Stokes shifts, and different lifetimes. We have reconciled the Stokes shift picture with Laenen's subband picture by showing how to determine the Stokes shifts of individual subbands and found that different subbands have different Stokes shifts. The peculiar properties of the smaller blue subband suggest that it represents water molecules with a broken hydrogen bond to one H atom, although this tentative structural interpretation needs to be confirmed by simulations.

Acknowledgements

This material is based on work supported by the National Science Foundation under Award No. DMR-0096466, by Army Research Office Contract DAAD19-00-1-0036 and by Air Force Office of Scientific Research Contract F49620-03-1-0032.

References

[1] A. Laubereau, W. Kaiser, Rev. Mod. Phys. 50 (1978) 607.
[2] D.D. Dlott, Chem. Phys. 266 (2001) 149.
[3] R. Laenen, C. Rauscher, A. Laubereau, J. Phys. Chem. B 102 (1998) 9304.
[4] R. Laenen, C. Rauscher, A. Laubereau, Phys. Rev. Lett. 80 (1998) 2622.
[5] S. Woutersen, H.J. Bakker, Phys. Rev. Lett. 83 (1999) 2077.
[6] G.M. Gale, G. Gallot, F. Hache, N. Lascoux, S. Bratos, J.-C. Leicknam, Phys. Rev. Lett. 82 (1999) 1068.
[7] S. Bratos, G.M. Gale, G. Gallot, F. Hache, N.N. Lascoux, J.-C. Leicknam, Phys. Rev. E 61 (2000) 5211.
[8] G. Gallot, N. Lascoux, G.M. Gale, J.-C. Leicknam, S. Bratos, S. Pommeret, Chem. Phys. Lett. 341 (2001) 535.
[9] J.C. Deàk, L.K. Iwaki, D.D. Dlott, J. Phys. Chem. 104 (2000) 4866.
[10] C.P. Lawrence, J.L. Skinner, J. Chem. Phys. 117 (2002) 5827.
[11] C.P. Lawrence, J.L. Skinner, Chem. Phys. Lett. 369 (2003) 472.
[12] C.P. Lawrence, J.L. Skinner, J. Chem. Phys. 118 (2003) 264.
[13] C.P. Lawrence, J.L. Skinner, J. Chem. Phys. 117 (2002) 8847.
[14] A. Piryatinski, C.P. Lawrence, J.L. Skinner, J. Chem. Phys. 118 (2003) 9664.
[15] A. Piryatinski, C.P. Lawrence, J.L. Skinner, J. Chem. Phys. 118 (2003) 9672.
[16] R. Rey, K.B. Møller, J.T. Hynes, J. Phys. Chem. A 106 (2002) 11993.
[17] M. Diraison, Y. Guissani, J.-C. Leicknam, S. Bratos, Chem. Phys. Lett. 258 (1996) 348.
[18] J.C. Deàk, L.K. Iwaki, S.T. Rhea, D.D. Dlott, J. Raman Spectrosc. 31 (2000) 263.

[19] A.J. Lock, H.J. Bakker, J. Chem. Phys. 117 (2002) 1708.
[20] A.J. Lock, S. Woutersen, H.J. Bakker, J. Phys. Chem. A 105 (2001) 1238.
[21] S. Woutersen, H.J. Bakker, Nature 402 (1999) 507.
[22] A. Pakoulev, Z. Wang, D.D. Dlott, Chem. Phys. Lett. 371 (2003) 594.
[23] A. Pakoulev, Z. Wang, Y. Pang, D.D. Dlott, 2003, unpublished.
[24] R. Rey, J.T. Hynes, J. Chem. Phys. 104 (1996) 2356.
[25] J.E. Bertie, Z. Lan, Appl. Spectrosc. 50 (1996) 1047.
[26] A. Rahman, F.H. Stillinger, J. Chem. Phys. 55 (1971) 3336.
[27] S. Woutersen, U. Emmerichs, H.J. Bakker, Science 278 (1997) 658.
[28] G.M. Gale, G. Gallot, N. Lascoux, Chem. Phys. Lett. 311 (1999) 123.
[29] R.W. Terhune, P.D. Maker, C.M. Savage, Phys. Rev. Lett. 14 (1965) 681.
[30] S. Woutersen, H.J. Bakker, J. Opt. Soc. Am. B 17 (2000) 827.
[31] S.A. Rice, in: P. Schuster et al. (Eds.), Topics in Current Chemistry, vol. 60, Springer, New York, 1975, p. 109.
[32] A. Luzar, J. Chem. Phys. 113 (2000) 10663.
[33] F.H. Stillinger, in: I. Prigogine, S.A. Rice (Eds.), Adv. Chem. Phys., vol. 31, Wiley, New York, 1975, p. 1.
[34] H. Xu, H.A. Stern, B.J. Berne, J. Phys. Chem. B 106 (2002) 2054.